



OPEN ACCESS

EDITED BY

T. Alexander Quinn,
Dalhousie University, Canada

REVIEWED BY

Roel Meiburg,
Maastricht University, Netherlands
Seiryu Sugiura,
UT-Heart Inc., Japan

*CORRESPONDENCE

Marina Strocchi,
marina.strocchi@kcl.ac.uk

SPECIALTY SECTION

This article was submitted to Cardiac
Electrophysiology,
a section of the journal
Frontiers in Physiology

RECEIVED 04 August 2022

ACCEPTED 29 August 2022

PUBLISHED 21 September 2022

CITATION

Strocchi M, Gillette K, Neic A, Elliott MK,
Wijesuriya N, Mehta V, Vigmond EJ,
Plank G, Rinaldi CA and Niederer SA
(2022), Comparison between
conduction system pacing and cardiac
resynchronization therapy in right
bundle branch block patients.
Front. Physiol. 13:1011566.
doi: 10.3389/fphys.2022.1011566

COPYRIGHT

© 2022 Strocchi, Gillette, Neic, Elliott,
Wijesuriya, Mehta, Vigmond, Plank,
Rinaldi and Niederer. This is an open-
access article distributed under the
terms of the [Creative Commons
Attribution License \(CC BY\)](https://creativecommons.org/licenses/by/4.0/). The use,
distribution or reproduction in other
forums is permitted, provided the
original author(s) and the copyright
owner(s) are credited and that the
original publication in this journal is
cited, in accordance with accepted
academic practice. No use, distribution
or reproduction is permitted which does
not comply with these terms.

Comparison between conduction system pacing and cardiac resynchronization therapy in right bundle branch block patients

Marina Strocchi^{1*}, Karli Gillette^{2,3}, Aurel Neic⁴, Mark K. Elliott^{1,5},
Nadeev Wijesuriya^{1,5}, Vishal Mehta^{1,5}, Edward J. Vigmond⁶,
Gernot Plank^{2,3}, Christopher A. Rinaldi^{1,5} and
Steven A. Niederer¹

¹School of Biomedical Engineering and Imaging Sciences, King's College London, London, United Kingdom, ²BioTechMed-Graz, Graz, Austria, ³Gottfried Schatz Research Center, Medical University of Graz, Graz, Austria, ⁴NumeriCor GmbH, Graz, Austria, ⁵Guy's and St Thomas' NHS Foundation Trust, London, United Kingdom, ⁶Lyric, University of Bordeaux, Bordeaux, France

A significant number of right bundle branch block (RBBB) patients receive cardiac resynchronization therapy (CRT), despite lack of evidence for benefit in this patient group. His bundle (HBP) and left bundle pacing (LBP) are novel CRT delivery methods, but their effect on RBBB remains understudied. We aim to compare pacing-induced electrical synchrony during conventional CRT, HBP, and LBP in RBBB patients with different conduction disturbances, and to investigate whether alternative ways of delivering LBP improve response to pacing. We simulated ventricular activation on twenty-four four-chamber heart geometries each including a His-Purkinje system with proximal right bundle branch block (RBBB). We simulated RBBB combined with left anterior and posterior fascicular blocks (LAFB and LPFB). Additionally, RBBB was simulated in the presence of slow conduction velocity (CV) in the myocardium, left ventricular (LV) or right ventricular (RV) His-Purkinje system, and whole His-Purkinje system. Electrical synchrony was measured by the shortest interval to activate 90% of the ventricles (BIVAT-90). Compared to baseline, HBP significantly improved activation times for RBBB alone (BIVAT-90: 66.9 ± 5.5 ms vs. 42.6 ± 3.8 ms, $p < 0.01$), with LAFB (69.5 ± 5.0 ms vs. 58.1 ± 6.2 ms, $p < 0.01$), with LPFB (81.8 ± 6.6 ms vs. 62.9 ± 6.2 ms, $p < 0.01$), with slow myocardial CV (119.4 ± 11.4 ms vs. 97.2 ± 10.0 ms, $p < 0.01$) or slow CV in the whole His-Purkinje system (102.3 ± 7.0 ms vs. 75.5 ± 5.2 ms, $p < 0.01$). LBP was only effective in RBBB cases if combined with anodal capture of the RV septum myocardium (BIVAT-90: 66.9 ± 5.5 ms vs. 48.2 ± 5.2 ms, $p < 0.01$). CRT significantly reduced activation times in RBBB in the presence of severely slow RV His-Purkinje CV (95.1 ± 7.9 ms vs. 84.3 ± 9.3 ms, $p < 0.01$) and LPFB (81.8 ± 6.6 ms vs. CRT: 72.9 ± 8.6 ms, $p < 0.01$). Both CRT and HBP were ineffective with severely slow CV in the LV His-Purkinje system. HBP is effective in RBBB patients with otherwise healthy myocardium and Purkinje system, while CRT and LBP are ineffective. Response to LBP improves when LBP is combined with RV septum

anodal capture. CRT is better than HBP only in patients with severely slow CV in the RV His-Purkinje system, while CV slowing of the whole His-Purkinje system and the myocardium favor HBP over CRT.

KEYWORDS

heart failure, dyssynchrony, conduction system pacing, cardiac resynchronization therapy, right bundle branch block, his bundle pacing, left bundle pacing

1 Introduction

Cardiac resynchronization therapy (CRT) is an effective treatment for heart failure (HF) patients with dyssynchrony. (Sieniewicz et al., 2019). Treatment is delivered with a right ventricular (RV) lead and a left ventricular (LV) lead implanted in a tributary of the coronary sinus (CS), normally targeting the latest activated region. Clinical trials consistently show that CRT benefits patients with left bundle branch block (LBBB). On the other hand, observational studies reported higher mortality rates in RBBB vs. LBBB patients following CRT (Auricchio et al., 2014). Regardless, between 9% and 13% of patients recruited in major CRT clinical trials have right bundle branch block (RBBB) (Salden O. A. E. et al., 2020).

Despite the lack of evidence of positive outcome in RBBB patients following CRT, (Henin et al., 2020) recent observational retrospective studies reported potential benefits in subgroups of the RBBB population. (Pastore et al., 2018). As CRT aims to correct LV activation delay, patients with concomitant LV activation delay and RBBB, manifesting as atypical RBBB, might still benefit from CRT. Pastore et al. (2018) reported that atypical RBBB led to response to CRT in 71.4% of cases, opposed to only 19.4% of cases in the presence of typical RBBB. Patients with RBBB concomitant with left anterior fascicular block (LAFB) or left posterior fascicular block (LPFB) might also potentially benefit from CRT, as an anterior or posterior block induces partially delayed LV activation (Naruse et al., 2014; Dennis et al., 2022). Identifying specific RBBB patient subgroups that will benefit from CRT remains an ongoing clinical challenge.

Conduction system pacing (CSP), delivered through His bundle (HBP) or left bundle pacing (LBP), has emerged as a valuable alternative treatment to standard CRT for LBBB patients (Lustgarten et al., 2015; Arnold et al., 2018). HBP has recently been applied to RBBB patients with impaired LV function with 95% success rates, with QRS narrowing achieved in 78% of patients (Sharma et al., 2018). However, HBP has the disadvantages of being technically challenging and requiring high pacing thresholds. LBP overcomes these issues, but it is often associated with RV delayed activation (Strocchi et al., 2020b). In RBBB patients with CRT indication, Vijayaraman et al. (2022) found that LBP led to moderate QRS narrowing, less so than with HBP. Nevertheless, RBBB correction and attenuation was observed in 33% and 64% of patients, respectively. The authors provided two hypotheses through

which LBP reduced RV delayed activation: 1) non-selective capture of the LBP stimulus or 2) anodal capture of the ring electrode, when this is in good contact with the RV side of the septum. Although several studies showed that CSP is an efficient CRT delivery method for LBBB patients, additional data is needed to understand the effect of CSP on RBBB patients.

We aim to study the effects of CRT, HBP, and LBP on different RBBB patient groups using computational models. Ventricular activation was simulated on twenty-four heart geometries generated from HF patients with CRT indication. We performed simulations in the presence of proximal RBBB combined with the following conduction disturbances: LAFB, LPFB, slow LV His-Purkinje system conduction velocity (CV), slow RV His-Purkinje system CV, slow His-Purkinje system CV in both ventricles and slow myocardium CV. We additionally tested the effect of non-selective LBP and selective LBP combined with anodal capture of the RV septum to test which approach results in correction or attenuation of the RBBB activation pattern.

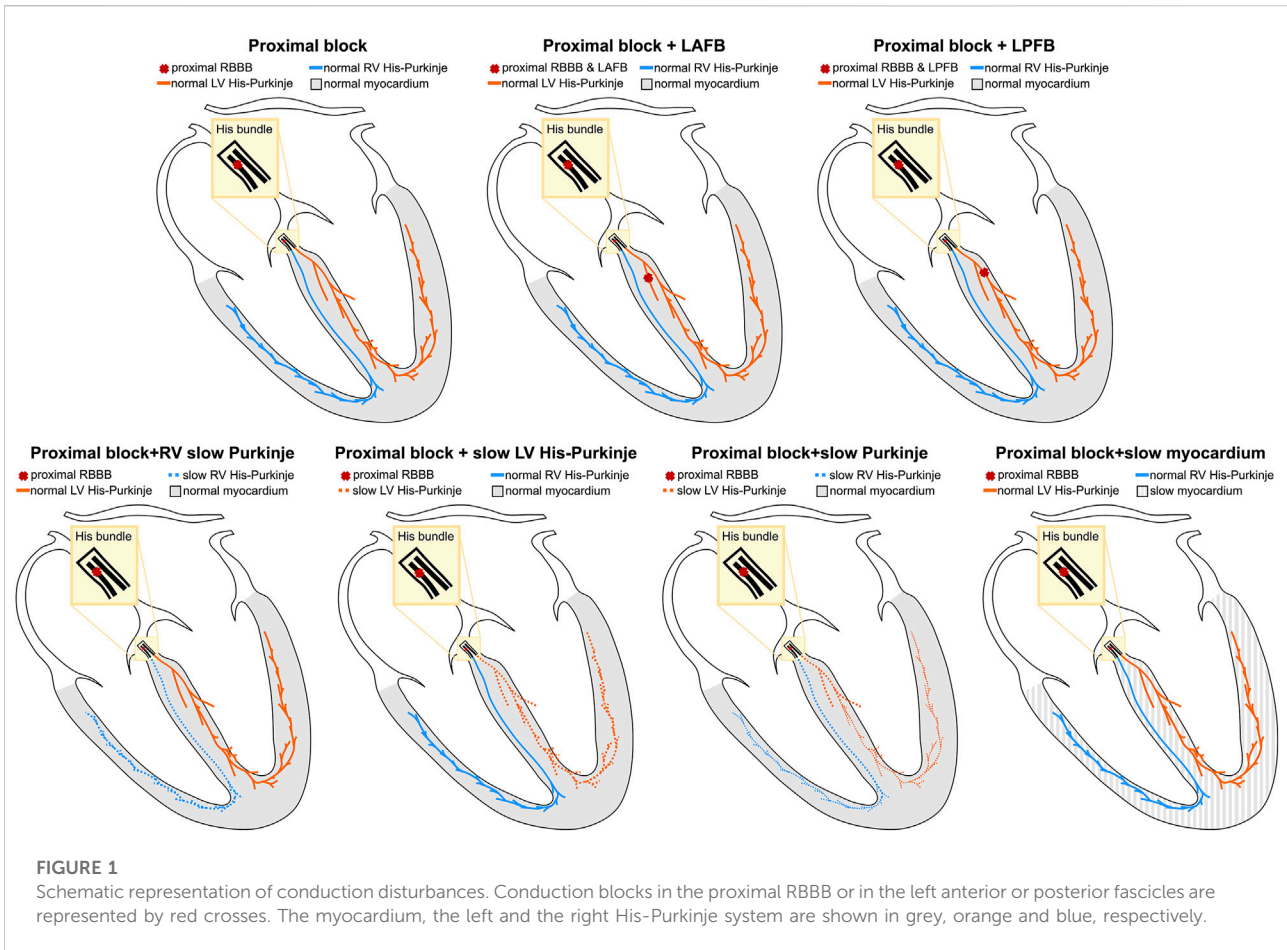
2 Materials and methods

We used twenty-four four-chamber heart tetrahedral meshes generated from HF patients as part of a previous study, with a mesh resolution of 1 mm (Strocchi et al., 2020a). Table 1 presents the patient cohort demographics, the LV, RV volume, and LV diameter derived from the mesh as described in (Strocchi et al., 2020a). A His-Purkinje network accounting for three LV fascicles (anterior and posterior, which further branches into two septal fascicles) and two RV fascicles (one septal fascicle and the moderator band) was

TABLE 1 Patient Characteristics. The table shows the characteristics of the twenty-four heart failure patients the meshes were derived from. The LV volume, the RV volume and the LV diameter were derived from the meshes. All quantities apart from the sex are presented as mean \pm standard deviation.

patient characteristics

Age [years]	67 \pm 14
Sex	23 Males, 1 Female
LV volume [ml]	269 \pm 78
RV volume [ml]	219 \pm 39
LV diameter [mm]	65 \pm 8



generated for each mesh as described previously (Gillette et al., 2021; Gillette et al., 2022). In the Supplement, we provide additional details about the construction of the His-Purkinje networks. Proximal RBBB was introduced by disconnecting the right bundle from the RV Purkinje system along the His. LAFB and LPFB were introduced by disconnecting the anterior and the posterior fascicle from the left bundle, respectively.

2.1 Electrophysiology simulations

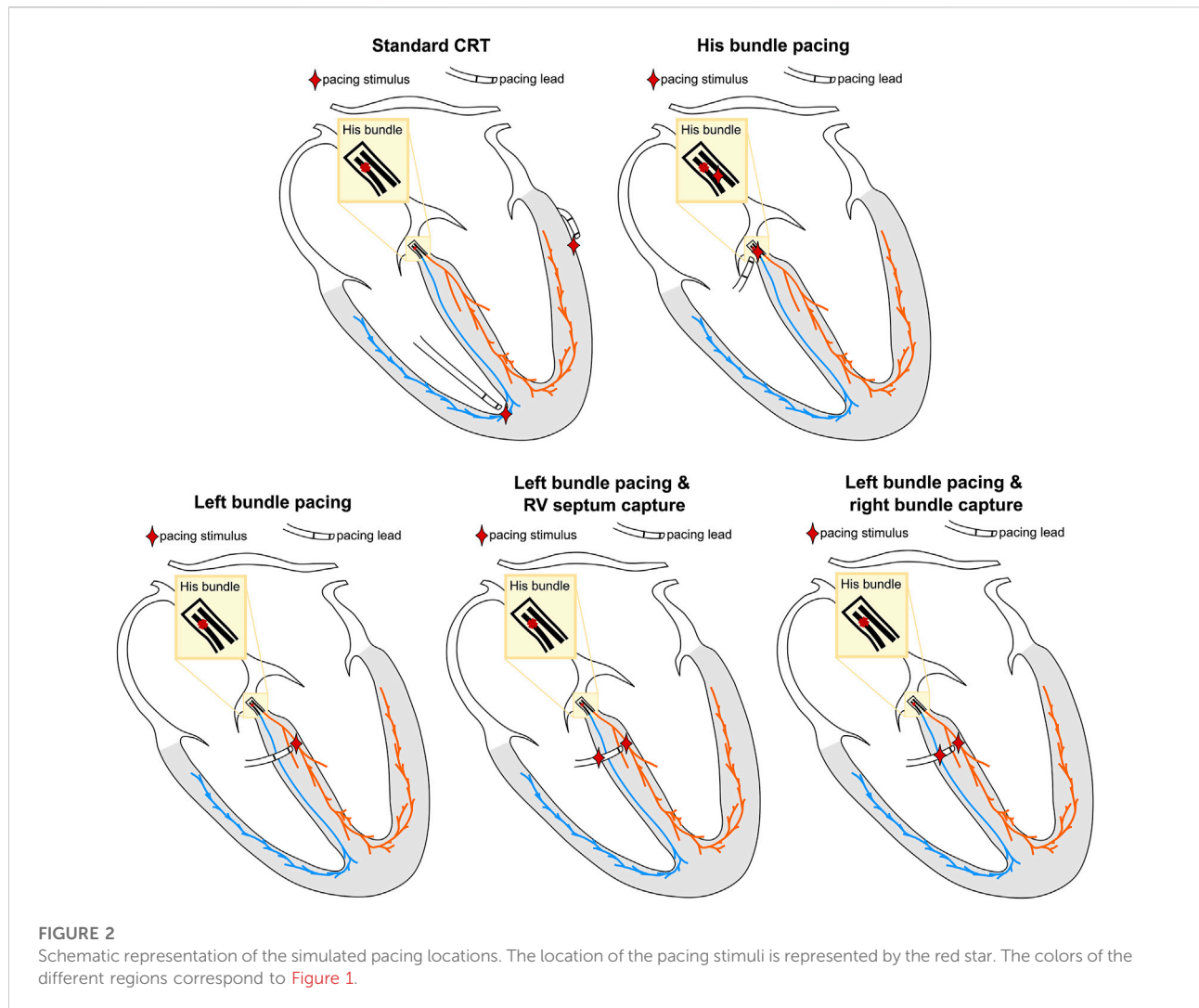
An Eikonal model was used to simulate ventricular electrical activation (Neic et al., 2017). The Eikonal model computes the local time $t_a(\mathbf{x})$ at each node with location \mathbf{x} within a domain Ω , provided an initial activation time t_0 at an initial stimulus location Γ and the CV tensor \mathbf{V} , containing the squared CV along the fiber, sheet and normal to sheet directions.

$$\sqrt{\nabla t_a(\mathbf{x})^T \mathbf{V} \nabla t_a(\mathbf{x})} = 1, \mathbf{x} \in \Omega$$

$$t_a(\mathbf{x}) = t_0, \mathbf{x} \in \Gamma$$

The myocardium was treated as a transversely isotropic medium, so the CV in the sheet and in the normal directions were set to be the same and are referred to as transverse CV. The CV of ventricular myocardium was set to 0.6 m/s and 0.24 m/s in the fiber and transverse directions, respectively. (Draper and Mya-Tu, 1959). The His-Purkinje system was assigned with a CV of 3.0 m/s (Ono et al., 2009). During sinus rhythm, the CV of each fascicle was tuned to achieve simultaneous activation of the end of the three LV fascicles, and activation of the end of the two RV fascicles 10 ms later than the LV fascicles, (Gillette et al., 2022) to replicate the Durrer maps (Durrer et al., 1970). The Eikonal equation was solved with the Fast Iterative Algorithm, as described in (Neic et al., 2017).

RBBB patients may present with additional conduction disturbances such as LAFB, LPFB (Naruse et al., 2014; Dennis et al., 2022), and His-Purkinje (Maguy et al., 2009) or myocardium CV slowing (Akar et al., 2004), which were both reported in the failing heart due to altered gap junction protein expression. To represent the heterogeneity of the RBBB population, we simulated the following scenarios: 1) proximal



RBBB and otherwise normal myocardium and His-Purkinje system; 2) proximal RBBB and LAFB; 3) proximal RBBB and LPFB; 4) proximal RBBB with mild or severe LV His-Purkinje CV slowing; 5) proximal RBBB with mild or severe RV His-Purkinje CV slowing; 6) proximal RBBB with mild or severe His-Purkinje CV slowing; 7) proximal RBBB with mild or severe myocardium CV slowing. Mild and severe CV slowing were simulated by reducing the CV down to 70% and 35% of reference CV values. [Figure 1](#) summarizes the different conduction disturbances we considered in this study. In the Supplement, we show the simulated activation times at baseline for proximal RBBB, and proximal RBBB concomitant with LAFB or LPFB for all twenty-four heart geometries. We then compare the simulated activation patterns and activation metrics against reported RBBB activation features and values in the literature, to show that the models are able to replicate RBBB activation patterns.

Selective HBP was simulated by pacing the His below the block, to simulate perfect correction of proximal RBBB. Selective

LBP was simulated by stimulating the left bundle. For non-selective LBP, the LBP stimulus was extended to the surrounding myocardium. Anodal capture of the RV septum during LBP was simulated by projecting the LBP stimulus site onto the RV septum. This site and the left bundle were then paced simultaneously. To investigate the difference between anodal capture of RV septum myocardium and distal right bundle anodal capture, we moved the RV septum stimulus to the closest point on the right bundle and paced simultaneously to selective and non-selective LBP. Finally, standard CRT was simulated by stimulating the RV at the apex and the LV at the latest activated region in the LV epicardium, with the RV-LV delay set to 0 ms. [Figure 2](#) shows a schematic representation of the pacing locations.

We quantified biventricular (BIV) synchrony using the 90% of biventricular activation time (BIVAT-90), computed as the shortest interval needed to activate 90% of the ventricles, and the biventricular dyssynchronous index (BIVDI), computed as the

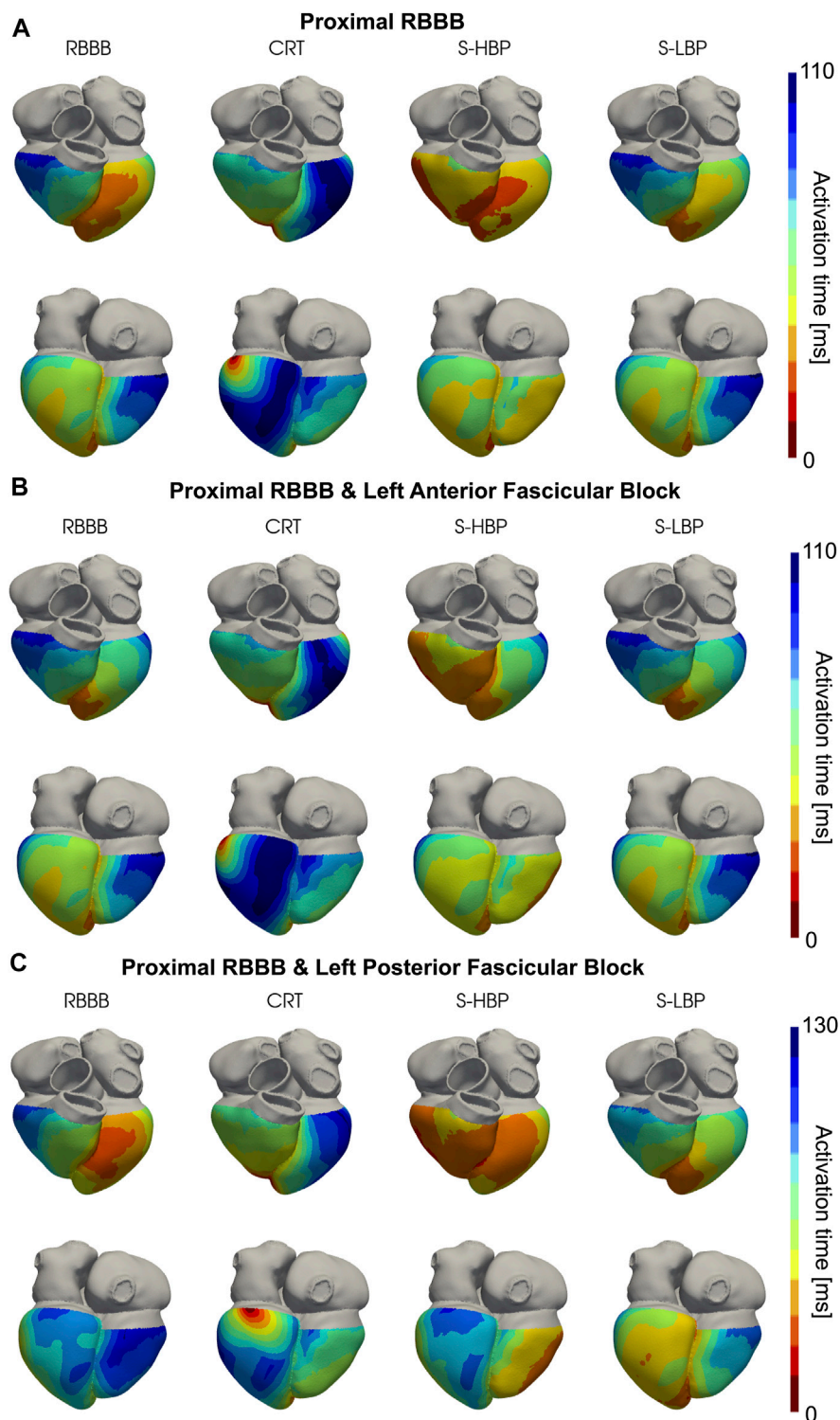


FIGURE 3

Simulated Activation Times: Activation times simulated on one of the patients for baseline, CRT, selective HBP (S-HBP) and selective LBP (S-LBP) in the presence of proximal RBBB combined with: **(A)** otherwise normal His-Purkinje system, **(B)** left anterior fascicular block and **(C)** left posterior fascicular block.

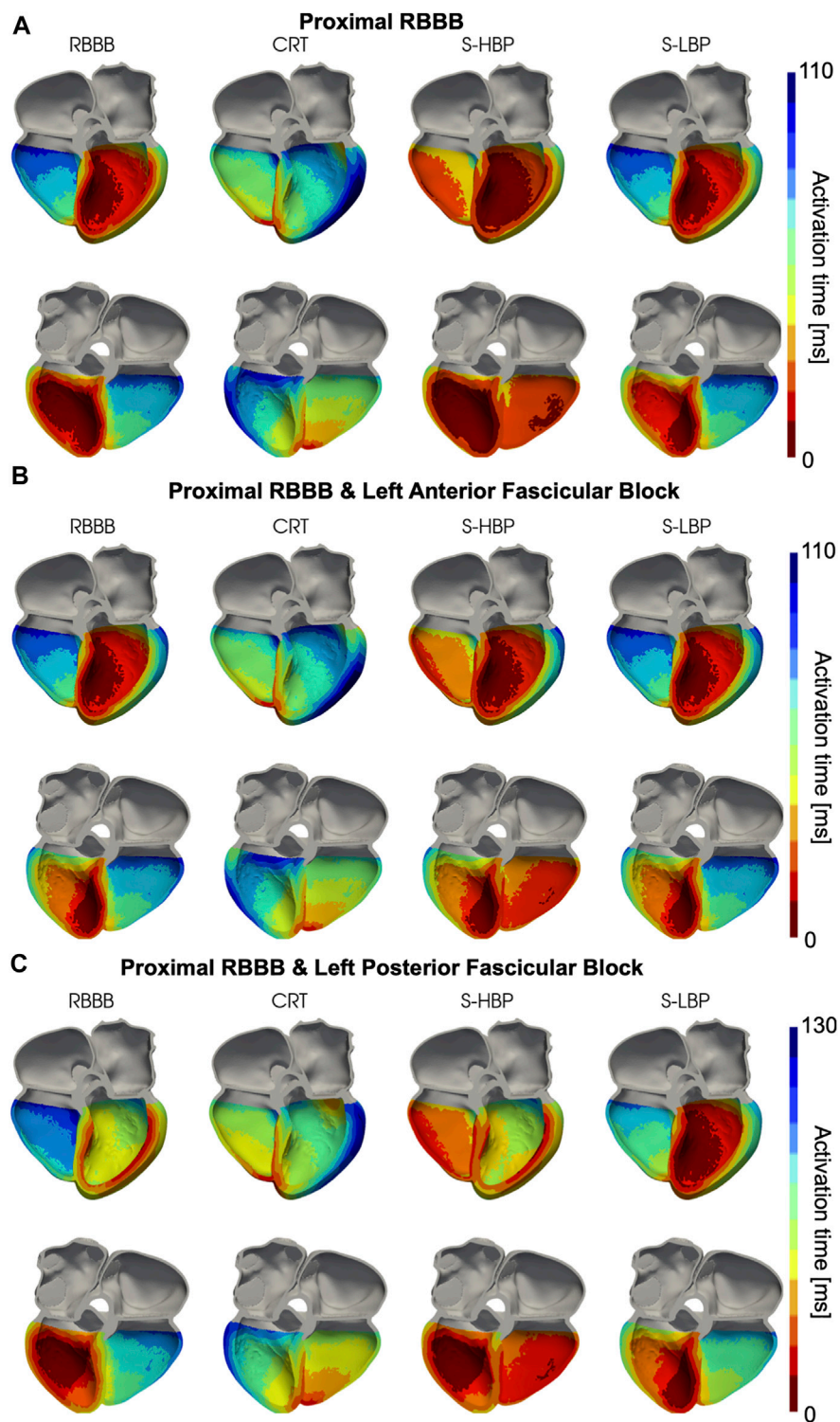
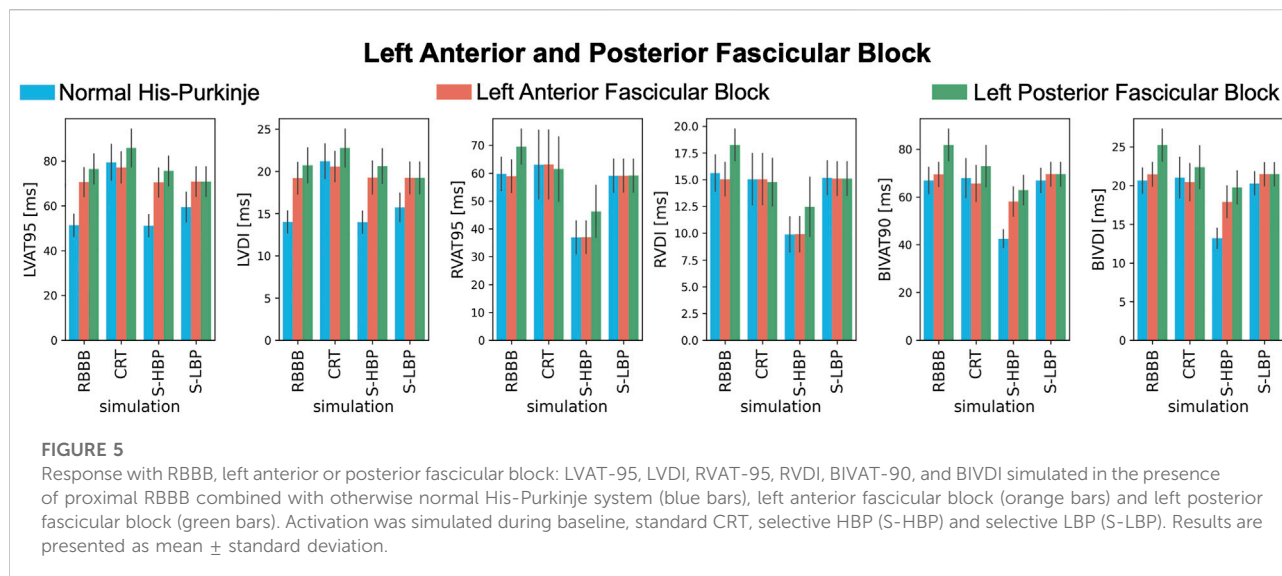


FIGURE 4

Simulated Activation Times (clipped view): Activation times simulated on one of the patients for baseline, CRT, selective HBP (S-HBP) and selective LBP (S-LBP) in the presence of proximal RBBB, shown on an anterior and a posterior clipped view of the mesh to show activation times. Proximal RBBB was combined with: **(A)** otherwise normal His-Purkinje system, **(B)** left anterior fascicular block and **(C)** left posterior fascicular block.



standard deviation of ventricular activation times. The BIVDI was computed accounting for the activation times of all nodes of the ventricles to quantify the dispersion of ventricular activation, based on clinical studies using activation time measurements from electrocardiographic imaging (Arnold et al., 2018) or an ECG belt (Salden F. C. W. M. et al., 2020). LV and RV synchrony were assessed by computing 95% of LV activation time (LVAT-95) and the LV dyssynchronous index (LVDI), and the 95% of RV activation time (RVAT-95) and the RV dyssynchronous index (RVDI), respectively. The peri-annular regions of the interventricular valves were excluded when computing activation times, while the septum was considered to be part of the LV when computing LV metrics.

2.2 Statistical analysis

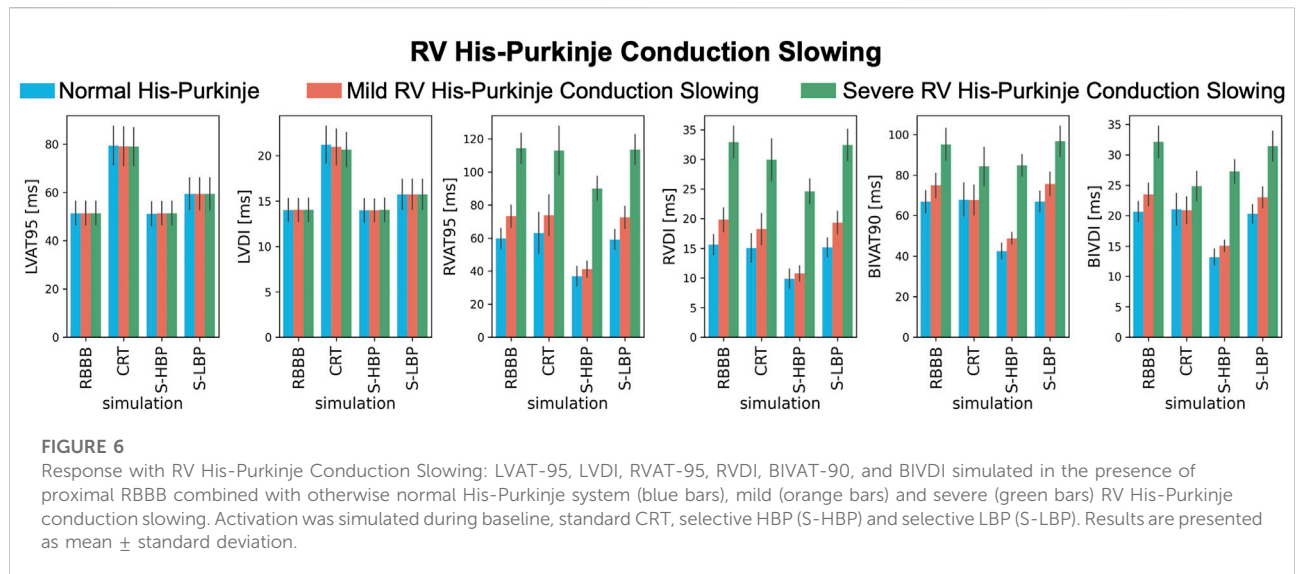
Simulation results were compared using one-way analysis of variance (ANOVA). Post-hoc comparison analysis was performed to see which pairwise comparisons were statistically different using the Tukey's honestly significant difference test.

3 Results

We simulated proximal RBBB with otherwise normal His-Purkinje system, and combined with LAFB or LPFB. Figures 3, 4 show the distribution of simulated activation times for these three different scenarios during baseline, standard CRT, selective HBP and selective LBP for one heart geometry, with red and blue areas representing early and late activated regions, respectively. RV delayed activation caused by RBBB at baseline with otherwise

healthy His-Purkinje conduction (Figure 3A), LAFB (Figure 3B) or LPFB (Figure 3C) was corrected by HBP. Septal activation, which during baseline occurs from left to right due to RBBB, is synchronized by HBP as the electrical propagation can travel along the right bundle, activating the RV septal fascicle and the RV moderator band (Figure 4, columns 1 and 3). On the other hand, CRT led to prolonged LV activation times in all three cases. Selective LBP preserved baseline RV delayed activation in the presence of proximal RBBB alone and RBBB combined with LAFB, while it improved activation when RBBB was concomitant with LPFB, because the LBP stimulus was placed downstream from the LPFB. Figure 4C shows that, at baseline, the posterior septum and the posterior LV free wall are activated late due to LPFB. As opposed to HBP, where late activation of the LV posterior septum is preserved, selective LBP is able to activate these areas early, leading to improved LV and RV activation.

These results are confirmed when comparing LV, RV, and BIV response metrics between baseline and pacing (Figure 5). During proximal RBBB alone (Figure 5, blue bars), selective HBP caused no change in LVAT-95 compared to baseline (51.3 ± 4.9 ms vs. 51.2 ± 4.9 ms, $p = 0.9$), while LVAT-95 got worse with CRT (79.4 ± 8.0 ms, $p < 0.01$). On the other hand, RVAT-95 remained unaltered by CRT (59.7 ± 6.0 ms vs. 63.1 ± 12.3 ms, $p = 0.76$) and improved with HBP (36.9 ± 5.8 ms, $p < 0.01$). BIVAT-90 was unaltered by CRT (66.9 ± 5.5 ms vs. 67.9 ± 8.2 ms, $p = 0.9$) and by selective LBP (66.9 ± 5.1 ms, $p = 0.9$) due to prolonged RV activation (RVAT-95: 59.1 ± 6.0 ms, $p = 0.9$ vs. baseline), while HBP shortened BIVAT-90 significantly (42.6 ± 3.8 ms, $p < 0.01$ vs. baseline). When RBBB was concomitant with LAFB (Figure 5, orange bars) or LPFB (Figure 5, green bars), LVAT-95 was worsened by CRT (RBBB + LAFB: 70.6 ± 6.4 ms vs. 77.2 ± 6.9 ms, $p < 0.01$; RBBB + LPFB: 76.5 ± 6.7 ms vs. 85.8 ± 8.5 ms, $p < 0.01$) but remained unchanged during HBP (RBBB + LAFB:

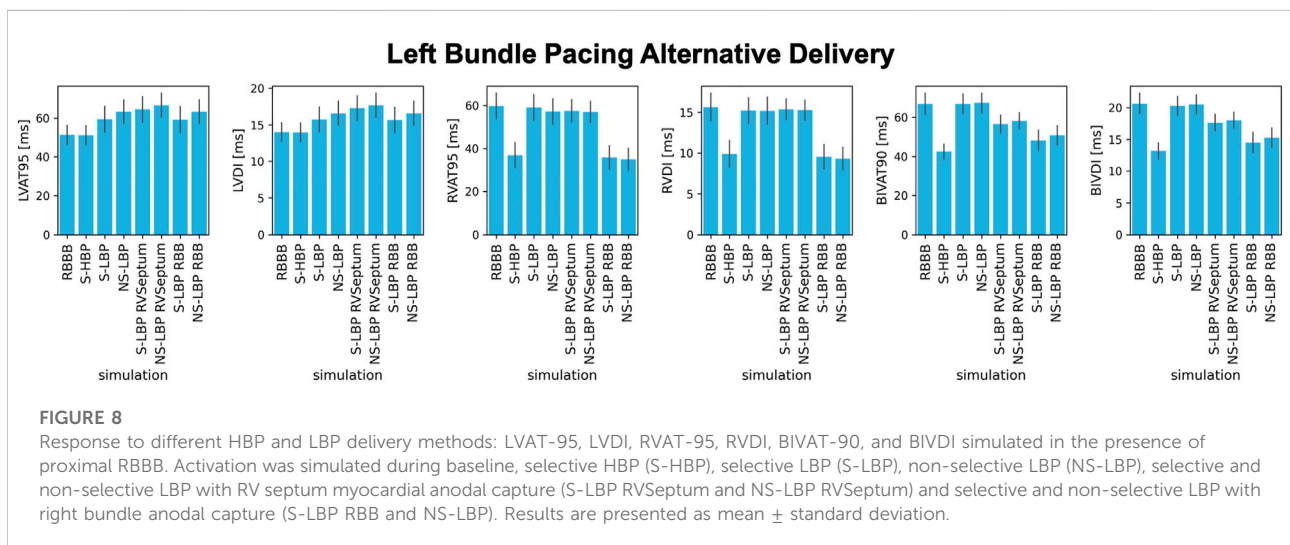


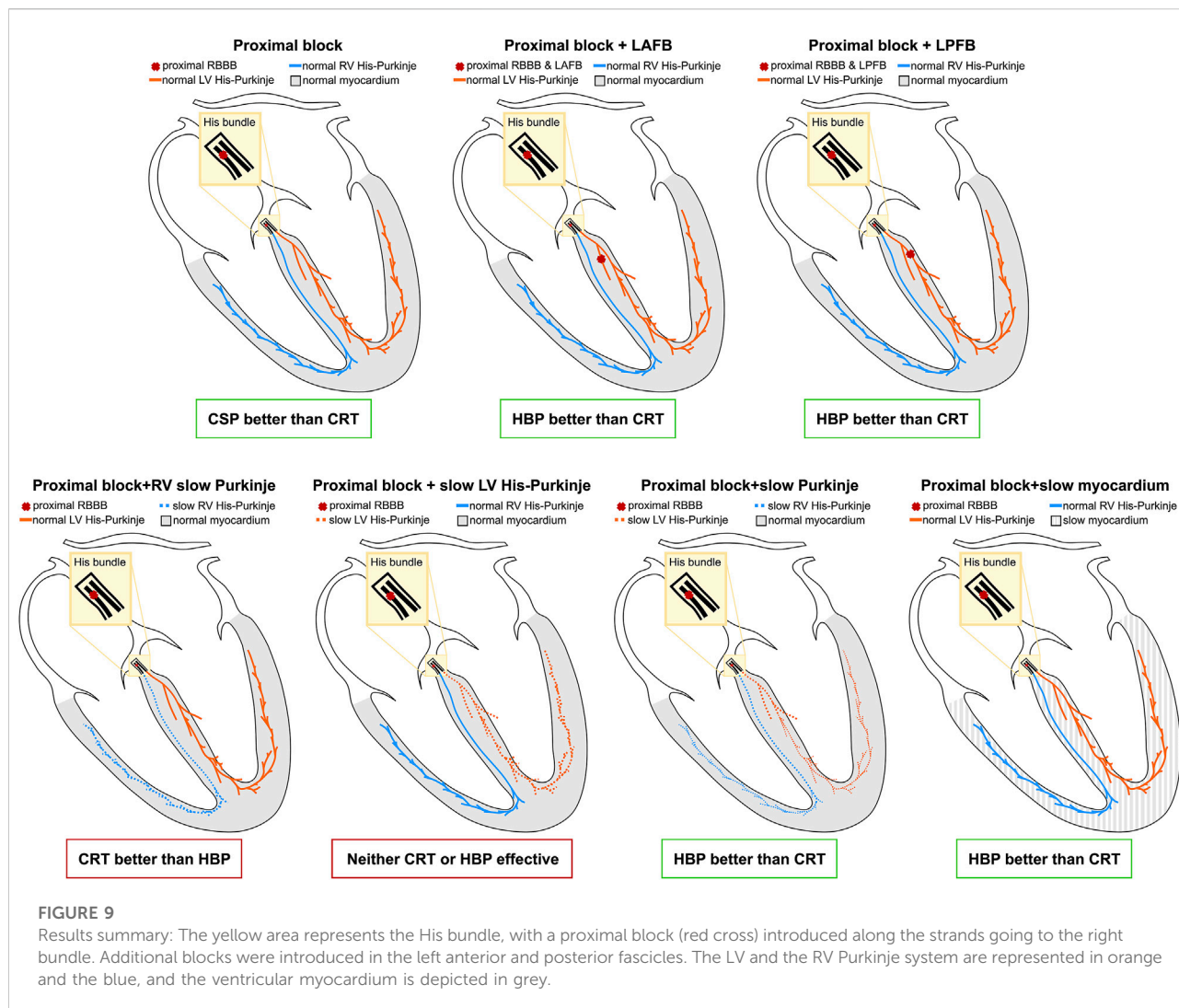
70.4 \pm 6.5 ms $P = 0.9$ vs. baseline; RBBB + LPFB: 75.6 \pm 6.6 ms $P = 0.9$ vs. baseline). Similar to proximal RBBB alone, in the presence of LAFB RVAT-95 was unaltered by CRT and selective LBP, and significantly improved by selective HBP. Selective LBP improved LVAT-95 (70.8 \pm 6.5 ms $P = 0.04$ vs. baseline) and RVAT-95 (59.2 \pm 5.9 ms, $p < 0.01$ vs. baseline) with RBBB and LPFB, although differences in LVAT-95 were not statistically significant. In this case, BIVAT-90 was improved significantly by all pacing modalities (baseline: 81.8 \pm 6.6 ms vs. CRT: 72.9 \pm 8.6 ms $P < 0.01$, HBP: 62.9 \pm 6.2 ms $P < 0.01$, LBP: 69.5 \pm 5.0 ms $P < 0.01$), but most significantly by HBP. HBP decreased BIVAT-90 with RBBB combined with LAFB as well (69.5 \pm 5.0 ms vs. 58.1 \pm 6.2 ms, $p < 0.01$), thanks to complete RBBB correction.

We investigated how mild and severe deterioration of RV His-Purkinje conduction properties affected response to pacing by reducing the RV His-Purkinje CV. Mild RV His-Purkinje conduction slowing combined with proximal RBBB (Figure 6, orange bars) favored HBP (74.9 \pm 6.0 ms vs. 48.8 \pm 2.8 ms, $p < 0.01$) over CRT, although CRT still shortened BIVAT-90 (67.7 \pm 7.4 ms, $p < 0.01$ vs. baseline). In the presence of severe RV His-Purkinje conduction slowing, CRT was effective at shortening BIVAT-90 (95.1 \pm 7.9 vs. 84.3 \pm 9.3 ms, $p < 0.01$) and RVDI (33.0 \pm 2.7 vs. 30.0 \pm 3.5 ms, $p < 0.01$), and was comparable to HBP (BIVAT-90: 84.8 \pm 5.2 ms, $p = 0.9$ vs. CRT). On the other hand, BIVDI was better with CRT than HBP (baseline: 32.1 \pm 2.6 ms vs. CRT: 24.9 \pm 2.4 ms vs. 27.3 \pm 1.9 ms). LBP was ineffective, as RV activation remained delayed in the presence of both mild (BIVAT90: 75.7 \pm 5.7 ms, $p = 0.9$ vs baseline) and severe (96.6 \pm 7.5 ms, $p = 0.9$ vs. baseline) RV His-Purkinje conduction slowing.

To test how alterations of conduction properties of the LV His-Purkinje system, the whole His-Purkinje system and the myocardium affected response to pacing, we simulated RBBB

combined with LV His-Purkinje system CV slowing, His-Purkinje system CV slowing and myocardium CV slowing (Figure 7). Patients with proximal RBBB and mild LV His-Purkinje conduction slowing (Figure 7A, orange bars) responded to HBP. BIVAT-90 and RVAT-95 were significantly better with HBP compared to baseline (BIVAT-90: 67.5 \pm 5.5 ms vs. 49.1 \pm 4.6 ms, $p < 0.01$; RVAT-95: 59.2 \pm 6.3 ms vs. 40.9 \pm 6.8 ms, $p < 0.01$), while LVAT-95 remained unaltered (59.1 \pm 5.6 ms vs. 59.4 \pm 5.6 ms, $p = 0.9$). CRT worsened both LVAT-95 (89.4 \pm 8.7 ms, $p < 0.01$) and BIVAT-90 (76.4 \pm 8.6 ms, $p < 0.01$) compared to baseline. CRT also led to worse LV, RV, and BIV activation in the presence of severe LV His-Purkinje conduction slowing (Figure 7, green bars). In this case, HBP was also ineffective, leading to longer LVAT-95 (87.6 \pm 7.9 ms vs. 113.4 \pm 8.7 ms, $p < 0.01$) and BIVAT-90 (75.2 \pm 6.1 ms vs. 94.5 \pm 10.5 ms, $p < 0.01$) compared to baseline, despite RV activation times were still shortened thanks to RBBB correction (RVAT-95: 57.8 \pm 7.1 ms vs. 46.8 \pm 9.7 ms, $p < 0.01$). When proximal RBBB was concomitant with mild (Figure 7B, orange bars) or severe (Figure 7B, green bars) conduction slowing of the whole His-Purkinje system, CRT worsened LVAT-95 from baseline, while BIVAT-90 and RVAT-95 remained unchanged. On the other hand, HBP remained effective at shortening BIVAT-90 (severe His-Purkinje conduction slowing: 102.3 \pm 7.0 ms vs. 75.5 \pm 5.2 ms, $p < 0.01$) and RVAT-95 (112.8 \pm 9.5 ms vs. 63.6 \pm 5.4 ms, $p < 0.01$). Similarly, HBP shortened BIV and RV activation in the presence of proximal RBBB, normal His-Purkinje conduction but mildly (BIVAT-90: 79.2 \pm 6.8 ms vs. 54.8 \pm 5.2, $p < 0.01$; RVAT-95: 65.8 \pm 7.3 ms vs. 48.2 \pm 8.3 ms, $p < 0.01$) or severely (BIVAT-90: 119.4 \pm 11.4 ms vs. 97.2 \pm 10.0 ms, $p < 0.01$; RVAT-95: 89.4 \pm 12.7 ms vs. 86.1 \pm 16.3 ms $P = 0.9$) slow myocardium (Figure 7C), although differences in RVAT-95





with severely slow myocardium were not statistically significant. On the other hand, in these cases, CRT worsened LVAT-95, RVAT-95, and BIVAT-90. In particular, BIVAT-90 was significantly increased during CRT compared to baseline in the presence of severe myocardium conduction slowing (CRT: 134.8 ± 24.3 ms, $p < 0.01$ baseline). CRT and LBP were ineffective in the presence of RBBB combined with mild or severe CV slowing affecting the LV His-Purkinje, the whole His-Purkinje or the myocardium. On the other hand, HBP was ineffective only when RBBB was concomitant with severe LV His-Purkinje CV slowing due to delayed LV activation, while it improved LV, RV, and BIV activation times in all other simulated scenarios.

In all cases apart from proximal RBBB combined with LPFB, selective LBP did not improve BIV activation times due to prolonged RV activation during pacing. We investigated whether non-selective capture of the left bundle, selective LBP and non-selective LBP combined with anodal capture of the RV septum or the right bundle improved RV activation. **Figure 8**

shows the results for proximal RBBB baseline, HBP and different delivery methods for LBP. Non-selective LBP was comparable to selective LBP in terms of all metrics ($p > 0.05$). It is however worth noting that, while not statistically significant, non-selective LBP prolongs LVAT-95 compared to selective LBP. This is because, with non-selective pacing, early activation starts in the septum travelling through the slow myocardium, rather than the Purkinje system alone, as opposed to selective LBP. On the other hand, BIVAT-90 were significantly shorter with selective LBP and anodal capture of the RV septum compared to baseline and selective and non-selective LBP alone (baseline: 66.9 ± 5.5 ms, S-LBP: 66.9 ± 5.1 ms vs. NS-LBP: 67.4 ± 5.0 ms vs. S-LBP + RV septum: 56.6 ± 4.5 ms, $p < 0.01$). Biventricular synchrony was also improved with RV septum anodal capture compared to selective and non-selective LBP alone (BIVDI: S-LBP: 20.3 ± 1.5 ms and NS-LBP: 20.5 ± 1.5 ms vs. S-LBP + RV septum: 17.6 ± 1.3 ms, $p < 0.01$). Anodal capture of the right bundle during selective LBP led to further improvements of

biventricular activation and synchrony. BIVAT-90 were 48.2 ± 5.2 ms and significantly shorter than baseline and selective LBP with RV septum anodal capture, due to significantly shorter RVAT-95 (35.9 ± 5.4 ms, $p < 0.01$ vs. baseline). BIV synchrony was also better compared to RV septum anodal capture (BIVDI: 14.5 ± 1.6 ms, $p < 0.01$ vs. LBP + RV septum capture), and comparable to selective HBP (BIVDI: HBP 13.2 ± 1.3 ms, $p = 0.13$). Non-selective LBP rather than selective capture during RV anodal capture did not affect any of the metrics ($p > 0.05$).

4 Discussion

We performed an in-silico electrophysiology clinical trial to study the effect of standard CRT, HBP, and LBP on RBBB patients. We simulated the presence of RBBB combined with different conduction disturbances to see how they altered response to pacing. [Figure 9](#) summarizes the results of our study. In patients with proximal RBBB and otherwise normal His-Purkinje system and myocardium, CRT and LBP were ineffective, while HBP improved activation. Similar observations applied when RBBB was combined with LAFB. On the other hand, patients with RBBB and LPFB responded to HBP, LBP and standard CRT, although HBP was still the most effective. Severe RV His-Purkinje conduction slowing combined with RBBB led to improved ventricular synchrony with CRT compared to HBP, while severe LV His-Purkinje conduction slowing made all pacing modalities ineffective due to severely prolonged LV activation. RBBB with slowed CV in the whole His-Purkinje system or the myocardium favored HBP over CRT, where LV and BIV activation were longer than baseline. We tested whether alternative ways of delivering LBP could improve RV activation and therefore improve overall ventricular synchrony. Non-selective LBP was comparable to selective LBP. On the other hand, selective LBP delivered in combination with anodal capture of the RV septum or the right bundle led to significantly improved ventricular activation compared to LBP alone.

Many large, multicenter clinical trials have proved that CRT is more effective in LBBB than RBBB patients. ([Hara et al., 2012](#); [Auricchio et al., 2014](#); [Pastore et al., 2018](#); [Henin et al., 2020](#)). Despite this, a large proportion of RBBB patients are delivered with CRT to attempt to treat dyssynchrony and improve cardiac function. In agreement with our study, [Pastore et al. \(2018\)](#) reported that patients with typical RBBB were less likely to respond to CRT compared to patients with atypical RBBB, where RBBB might mask some additional dyssynchrony. For instance, RBBB patients with LV dyssynchrony were shown to benefit from CRT, while in patients with RBBB and no or small LV dyssynchrony, CRT prolonged LV activation. ([Salden O. A. E. et al., 2020](#)). Our simulations show that only in presence of RBBB and LPFB or severely slow RV His-Purkinje conduction slowing, CRT improved BIV activation, while all other types of

dyssynchrony did not favor CRT. Our results explain the variation in outcomes in patients with RBBB, and provide insight into which RBBB patient subgroups are likely to respond to CRT.

HBP is emerging as an alternative way of delivering CRT in patients where standard CRT is not feasible or ineffective. HBP safety and efficacy has been investigated and confirmed by small clinical trials on LBBB patients, ([Lustgarten et al., 2015](#); [Arnold et al., 2018](#)), while there is a lack of data on the effect of HBP in the presence of RBBB. Nevertheless, if the site of block is proximal enough, HBP theoretically represents the most physiological method to deliver resynchronization in RBBB patients, potentially leading to perfect correction of RBBB morphology. [Sharma et al. \(2018\)](#) reported significant QRS narrowing in RBBB patients following successful delivery of HBP, consistent with our results. Despite these promising preliminary results, future efforts to investigate feasibility of HBP on RBBB patients are needed to extend HBP delivery to non-LBBB patient groups, with particular care in identifying dyssynchronies that are less likely to favor HBP efficacy.

LBP can be used as an alternative to HBP, when HBP cannot be delivered or requires high pacing thresholds to correct delayed LV activation in LBBB patients. Clinical and computational studies have shown that LBP can be as effective as HBP when AV delay optimization is possible, aiming to shorten RV activation times through the patient's intrinsic activation travelling down the viable fibers of the right bundle. ([Strocchi et al., 2020b](#); [Lin et al., 2020](#)). This is however not possible in RBBB patients. In agreement with our study, [Vijayarajan et al. \(2022\)](#) showed that LBP led to small changes in QRS duration (from 156 ± 20 ms to 150 ± 24 ms) in RBBB patients. On the other hand, HBP led to significant QRS narrowing. The authors however also reported that 33% of patients had complete RBBB correction following LBP, attributing this to two potential factors: non-selective LBP or anodal capture of the RV septum. Our simulations show that, while non-selective LBP would not explain improved RV activation compared to selective LBP, anodal capture of the RV septum during LBP could cause RBBB partial correction, with additional benefits induced by anodal capture of the right bundle. These results could be of particular interest with the advancement of leadless pacing. The Wise-CRT system (EBR Systems Inc., Sunnyvale CA) is a commercially available LV leadless pacing system that requires the co-implant of an RV lead delivering continuous pacing ([Wijesuriya et al., 2022](#)). Our results suggest that, by placing the RV lead in the RV septum potentially targeting the right bundle while delivering LBP through the leadless electrode, the Wise-CRT system could benefit RBBB patients. Although LBP alone might not constitute a viable method to deliver CRT in RBBB patients, its delivery could still be adapted and extended to this patient group.

4.1 Limitations

Although in-silico trials provide a systematic comparison between different CRT delivery methods, they rely on models with limitations. We assume that acute electrical response implies long-term benefits. Additional factors might affect response to therapy, but a review of CRT clinical trials showed that QRS narrowing was more significant in responders compared to non-responders (Bryant et al., 2013). Nevertheless, a future computational study considering mechanical as well as electrical synchrony induced by pacing would be of great interest, and might provide additional information about functional response to CRT. Furthermore, when simulating HBP, we assume perfect correction of RBBB through selective capture, while a proportion of patients are delivered with non-selective HBP, with clinical trials reporting selective capture achieved in between 6% and 100% of patients (Lewis et al., 2019). Therefore, our results might overestimate the electrical synchrony induced by HBP. We have performed simulations with non-selective HBP for all conduction disturbances, and provided a comparison with selective HBP in Section 3 of the Supplement. Non-selective pacing was equivalent to selective pacing for all patient groups but RBBB combined with LPFB and with severely slow His-Purkinje system. Nevertheless, early activation of the area around the His bundle might lead to changes in strains, therefore affecting mechanical synchrony, that this study does not account for.

Our models include synthetically generated His-Purkinje systems that did not replicate the conduction system of a specific patient. Nevertheless, we were able to simulate the main features of RBBB activation, as shown in the Supplement.

Finally, we simulated only ventricular activation times without propagation of the electrical activation in the torso, therefore not providing simulated surface ECGs. However, the torso geometries were not available for these patients. Therefore, simulating ECGs with sufficient accuracy would constitute a challenge that was outside the scope of this study.

Regardless of its limitations, our computational study provides a systematic comparison between different pacing modalities in the presence of RBBB combined with different conduction disturbances, showing which RBBB subgroups could respond to CRT, HBP, and LBP.

5 Conclusion

Patients with RBBB significantly benefit from HBP but not CRT or LBP, which preserves delayed RV activation. LBP delivered in combination with anodal capture of the RV septum shortens RV activation, leading to overall improved synchrony. When RBBB is concomitant with LPFB, CRT improves activation, but HBP is still more effective thanks to RBBB correction. Severely slow RV His-Purkinje CV with

proximal RBBB favors CRT over HBP, while severely slow LV His-Purkinje CV makes both CRT and HBP ineffective. When conduction slowing affects the whole His-Purkinje system or the ventricular myocardium, HBP is more effective than CRT.

Data availability statement

The raw data supporting the conclusion of this article will be made available by the authors, without undue reservation.

Author contributions

MS, SN, CR, ME, VM, and NW contributed to conception and design of the study. KG, GP, EJV and AN implemented the software used to run simulations. MS wrote the first draft of the manuscript, ran simulations and analyzed the results. All authors contributed to manuscript revision and approved the final submitted version.

Funding

This work was supported by the Wellcome/EPSRC Centre for Medical Engineering (WT 203148/Z/16/Z). SN is supported by NIH R01-HL152256, ERC PREDICT-HF 453 (864055), BHF (RG/20/4/34803), EPSRC (EP/P01268X/1).

Conflict of interest

Author AN is employed by NumeriCor GmbH, Graz, Austria.

The remaining authors declare that the research was conducted in the absence of any commercial or financial relationships that could be construed as a potential conflict of interest.

Publisher's note

All claims expressed in this article are solely those of the authors and do not necessarily represent those of their affiliated organizations, or those of the publisher, the editors and the reviewers. Any product that may be evaluated in this article, or claim that may be made by its manufacturer, is not guaranteed or endorsed by the publisher.

Supplementary material

The Supplementary Material for this article can be found online at: <https://www.frontiersin.org/articles/10.3389/fphys.2022.1011566/full#supplementary-material>

References

- Akar, F. G., Spragg, D. D., Tunin, R. S., Kass, D. A., and Tomaselli, G. F. (2004). Mechanisms underlying conduction slowing and arrhythmogenesis in nonischemic dilated cardiomyopathy. *Circ. Res.* 95, 717–725. doi:10.1161/01.RES.0000144125.61927.1c
- Arnold, A. D., Shun-Shin, M. J., Keene, D., Howard, J. P., Afzal Sohaib, S. M., Wright, I. J., et al. (2018). His resynchronization therapy vs. biventricular pacing for heart failure with LBBB: A within-patient comparison of effects on acute haemodynamic function and ventricular activation. *EP Europace* 20 (4), iv25. doi:10.1093/europace/euy201.001
- Auricchio, A., Lumens, J., and Prinzen, F. W. (2014). Does cardiac resynchronization therapy benefit patients with right bundle branch block? Cardiac resynchronization therapy has a role in patients with right bundle branch block. *Circ. Arrhythm. Electrophysiol.* 7, 532–542. doi:10.1161/CIRCEP.113.000628
- Bryant, A. R., Wilton, S. B., Lai, M. P., and Exner, D. v. (2013). Association between QRS duration and outcome with cardiac resynchronization therapy: A systematic review and meta-analysis. *J. Electrocardiol.* 46, 147–155. doi:10.1016/j.jelectrocard.2012.12.003
- Dennis, M. J., Sparks, P. B., and Capitani, G. (2022). Tailoring cardiac resynchronization therapy to non-left bundle branch block: Successful cardiac resynchronization for right bundle branch block with left posterior fascicular block without implantation of a left ventricular lead. *Indian Pacing Electrophysiol. J.* 22, 207–211. doi:10.1016/j.ipej.2022.04.002
- Draper, M. H., and Mya-Tu, M. (1959). A comparison of the conduction velocity in cardiac tissues of various mammals. *Q. J. Exp. Physiol. Cogn. Med. Sci.* 44, 91–109. doi:10.1113/expphysiol.1959.sp001379
- Durrer, D., van Dam, R. T., Freud, G. E., Janse, M. J., Meijler, F. L., and Arzbacher, R. C. (1970). Total excitation of the isolated human heart. *Circulation* 41, 899–912. doi:10.1161/01.CIR.41.6.899
- Gillette, K., Gsell, M. A. F., Bouyssier, J., Prassl, A. J., Neic, A., Vigmond, E. J., et al. (2021). Automated framework for the inclusion of a his–purkinje system in cardiac digital twins of ventricular electrophysiology. *Ann. Biomed. Eng.* 49, 3143–3153. doi:10.1007/s10439-021-02825-9
- Gillette, K. K., Gsell, M. A. F., Neic, A., Manninger, M., Scherr, D., Roney, C. H., et al. (2022). A personalized real-time virtual model of whole heart electrophysiology. *Front. Physiology*. (Under review). doi:10.3389/fphys.2022.907190
- Hara, H., Oyenuga, O. A., Tanaka, H., Adelstein, E. C., Onishi, T., McNamara, D. M., et al. (2012). The relationship of QRS morphology and mechanical dyssynchrony to long-term outcome following cardiac resynchronization therapy. *Eur. Heart J.* 33, 2680–2691. doi:10.1093/eurheartj/ehs013
- Henin, M., Ragy, H., Mannion, J., David, S., Refla, B., and Boles, U. (2020). Indications of cardiac resynchronization in non-left bundle branch block: Clinical review of available evidence. *Cardiol. Res.* 11, 1–8. doi:10.14740/cr989
- Lewis, A. J. M., Foley, P., Whinnett, Z., Keene, D., and Chandrasekaran, B. (2019). His bundle pacing: A new strategy for physiological ventricular activation. *J. Am. Heart Assoc.* 8, e010972. doi:10.1161/JAHA.118.010972
- Lin, J., Dai, Y., Wang, H., Li, Y., Chen, K., and Zhang, S. (2020). A comparison of left bundle branch pacing with His bundle pacing in a patient with heart failure and left bundle branch block. *Hear. Case Rep.* 6, 293–296. doi:10.1016/j.hrcr.2019.10.007
- Lustgarten, D. L., Crespo, E. M., Arkhipova-Jenkins, I., Lobel, R., Winget, J., Koehler, J., et al. (2015). His-bundle pacing versus biventricular pacing in cardiac resynchronization therapy patients: A crossover design comparison. *Heart rhythm.* 12, 1548–1557. doi:10.1016/j.hrthm.2015.03.048
- Maguy, A., le Bouter, S., Comtois, P., Chartier, D., Villeneuve, L., Wakili, R., et al. (2009). Ion channel subunit expression changes in cardiac purkinje fibers: A potential role in conduction abnormalities associated with congestive heart failure. *Circ. Res.* 104, 1113–1122. doi:10.1161/circresaha.108.191809
- Naruse, Y., Seo, Y., Murakoshi, N., Ishizu, T., Sekiguchi, Y., and Aonuma, K. (2014). Triventricular pacing improved dyssynchrony in heart failure patient with right-bundle branch block and left anterior fascicular block. *J. Cardiol. Cases* 9, 158–161. doi:10.1016/j.jccase.2013.12.013
- Neic, A., Campos, F. O., Prassl, A. J., Niederer, S. A., Bishop, M. J., Vigmond, E. J., et al. (2017). Efficient computation of electrograms and ECGs in human whole heart simulations using a reaction-eikonal model. *J. Comput. Phys.* 346, 191–211. doi:10.1016/j.jcp.2017.06.020
- Ono, N., Yamaguchi, T., Ishikawa, H., Arakawa, M., Takahashi, N., Saikawa, T., et al. (2009). Morphological varieties of the purkinje fiber network in mammalian hearts, as revealed by light and electron microscopy. *Arch. Histol. Cytol.* 72, 139–149. doi:10.1679/aohc.72.139
- Pastore, G., Morani, G., Maines, M., Marcantoni, L., Bolzan, B., Zanon, F., et al. (2018). Patients with right bundle branch block and concomitant delayed left ventricular activation respond to cardiac resynchronization therapy. *Europace* 20, e171–e178. doi:10.1093/europace/eux362
- Salden, F. C. W. M., Luermans, J. G. L. M., Westra, S. W., Weijts, B., Engels, E. B., Heckman, L. I. B., et al. (2020). Short-term hemodynamic and electrophysiological effects of cardiac resynchronization by left ventricular septal pacing. *J. Am. Coll. Cardiol.* 75, 347–359. doi:10.1016/j.jacc.2019.11.040
- Salden, O. A. E., Vernooy, K., van Stipdonk, A. M. W., Cramer, M. J., Prinzen, F. W., and Meine, M. (2020). Strategies to improve selection of patients without typical left bundle branch block for cardiac resynchronization therapy. *JACC. Clin. Electrophysiol.* 6, 129–142. doi:10.1016/j.jacep.2019.11.018
- Sharma, P. S., Naperkowski, A., Bauch, T. D., Chan, J. Y. S., Arnold, A. D., Whinnett, Z. I., et al. (2018). Permanent his bundle pacing for cardiac resynchronization therapy in patients with heart failure and right bundle branch block. *Circ. Arrhythm. Electrophysiol.* 11, e006613. doi:10.1161/CIRCEP.118.006613
- Sieniewicz, B. J., Gould, J., Porter, B., Sidhu, B. S., Teall, T., Webb, J., et al. (2019). Understanding non-response to cardiac resynchronization therapy: Common problems and potential solutions. *Heart Fail. Rev.* 24, 41–54. doi:10.1007/s10741-018-9734-8
- Strocchi, M., Augustin, C. M., Gsell, M. A. F., Karabelas, E., Neic, A., Gillette, K., et al. (2020a). A publicly available virtual cohort of fourchamber heart meshes for cardiac electromechanics simulations. *PLoS One* 15, e0235145. doi:10.1371/journal.pone.0235145
- Strocchi, M., Gillette, K. K., Neic, A., Elliott, M. K., Wijesuriya, N., Mehta, V., et al. (2022). The effect of scar and his-purkinje and myocardium conduction on response to conduction system pacing. *J. Am. Coll. Cardiol. Clin. Electrophysiol.* (Under review).
- Strocchi, M., Lee, A. W. C., Neic, A., Bouyssier, J., Gillette, K., Plank, G., et al. (2020b). His-bundle and left bundle pacing with optimized atrioventricular delay achieve superior electrical synchrony over endocardial and epicardial pacing in left bundle branch block patients. *Heart rhythm.* 17, 1922–1929. doi:10.1016/j.hrthm.2020.06.028
- Vijayaraman, P., Cano, O., Ponnusamy, S. S., Molina-Lerma, M., Chan, J. Y. S., Padala, S. K., et al. (2022). Left bundle branch area pacing in patients with heart failure and right bundle branch block: Results from International LBBAP Collaborative-Study Group. *Heart Rhythm O2* 3, 358–367. doi:10.1016/j.hroo.2022.05.004
- Wijesuriya, N., Elliott, M. K., Mehta, V., Sidhu, B. S., Behar, J. M., Niederer, S., et al. (2022). Leadless left ventricular endocardial pacing for cardiac resynchronization therapy: A systematic review and meta-analysis. *Heart rhythm.* 19, 1176–1183. doi:10.1016/j.hrthm.2022.02.018